Monthly Notices
of the
ROYAL ASTRONOMICAL SOCIETY

MNRAS **504,** 5671–5684 (2021) doi:10.1093/mnras/staa1245
Advance Access publication 2020 May 7

Original Research by Young Twinkle Students (ORBYTS): ephemeris refinement of transiting exoplanets

Billy Edwards ,[1]★ Quentin Changeat,[1] Kai Hou Yip,[1] Angelos Tsiaras,[1] Jake Taylor ,[2] Bilal Akhtar,[3] Josef AlDaghir,[3] Pranup Bhattarai,[3] Tushar Bhudia,[4] Aashish Chapagai,[3] Michael Huang,[3] Danyaal Kabir,[4] Vieran Khag,[4] Summyyah Khaliq,[4] Kush Khatri,[3] Jaidev Kneth,[4] Manisha Kothari,[4] Ibrahim Najmudin,[3] Lobanaa Panchalingam,[4] Manthan Patel,[3] Luxshan Premachandran,[4] Adam Qayyum,[4] Prasen Rana,[3] Zain Shaikh,[3] Sheryar Syed,[4] Harnam Theti,[4] Mahmoud Zaidani,[3] Manasvee Saraf,[1] Damien de Mijolla,[1] Hamish Caines,[1] Anatasia Kokori,[5,6] Marco Rocchetto,[1,7] Matthias Mallonn,[8] Matthieu Bachschmidt,[9] Josep M. Bosch,[10] Marc Bretton,[11] Philippe Chatelain,[12] Marc Deldem,[13] Romina Di Sisto,[14,15] Phil Evans,[16,17] Eduardo Fernández-Lajús,[14,15] Pere Guerra,[18] Ferran Grau Horta,[19] Wonseok Kang,[20] Taewoo Kim,[20] Arnaud Leroy,[21] František Lomoz,[22] Juan Lozano de Haro,[23] Veli-Pekka Hentunen,[24] Yves Jongen,[25] David Molina,[26] Romain Montaigut,[21] Ramon Naves,[27] Manfred Raetz,[28] Thomas Sauer,[29] Americo Watkins,[30] Anaël Wünsche,[11] Martin Zibar,[31] William Dunn,[1] Marcell Tessenyi,[1,32] Giorgio Savini,[1,32,33] Giovanna Tinetti[1,32] and Jonathan Tennyson [1,32]

Affiliations are listed at the end of the paper

Accepted 2020 April 29. Received 2020 March 19; in original form 2019 August 23

ABSTRACT

We report follow-up observations of transiting exoplanets that have either large uncertainties (>10 min) in their transit times or have not been observed for over 3 yr. A fully robotic ground-based telescope network, observations from citizen astronomers, and data from *TESS* have been used to study eight planets, refining their ephemerides and orbital data. Such follow-up observations are key for ensuring accurate transit times for upcoming ground- and space-based telescopes, which may seek to characterize the atmospheres of these planets. We find deviations from the expected transit time for all planets, with transits occurring outside the 1σ uncertainties for seven planets. Using the newly acquired observations, we subsequently refine their periods and reduce the current predicted ephemeris uncertainties to 0.28–4.01 min. A significant portion of this work has been completed by students at two high schools in London as part of the Original Research By Young Twinkle Students (ORBYTS) programme.

Key words: Exoplanets – Transits – Ephemerides – Orbital Parameters – Citizen Science – Outreach.

1 INTRODUCTION

Over the past decade, thousands of exoplanets have been detected via the transit method. Current and future observatories such as the *Transiting Exoplanet Survey Satellite* (*TESS*; Ricker et al. (2014) and the PLAnetary Transits and Oscillations of stars (PLATO; Rauer et al. 2016) satellite are expected to discover tens of thousands more. Upcoming ground- and space-based telescopes, such as the European Extremely Large Telescope (E-ELT; Brandl et al. 2018), the Thirty Meter Telescope (TMT; Skidmore, Anupama & Srianand 2018), the Giant Magellan Telescope (GMT; Fanson et al. (2018), the *James Webb Space Telescope* (*JWST*; Greene et al. 2016), *Twinkle* (Edwards et al. 2019c), and *Ariel* (Tinetti et al. 2018), will characterize the atmospheres of a large population of exoplanets via transit and eclipse spectroscopy at visible and infrared wavelengths. These missions will move the exoplanet field from an era of detection into one of characterization, allowing for the identification of the molecular species present and their chemical profile, insights into the atmospheric temperature profile, and the detection and characterization of clouds (e.g. Rocchetto et al. 2016; Rodler 2018; Changeat et al. 2019; Kawashima, Hu & Ikoma 2019). However, observing time on these exceptional facilities will be precious. Therefore observations of transiting exoplanets will need to have a limited time window while ensuring that enough margin is included to avoid a transit event being partially, or completely, missed. Large errors in the ephemerides of a planet increase the observation time required to ensure the full transit is captured and thus reduce the efficiency, and science yield, of these missions. Accurate ephemeris data, collected over a long baseline, can also be used to search for, and characterise, other planets in the system via transit time variations.

★ E-mail: billy.edwards.16@ucl.ac.uk

Just after discovery, the time of the next transit for a planet is well known. Unfortunately, the accuracy of predicted future transits degrades over time due to the increased number of epochs since the last observation and the stacking of the period error. In extreme cases, this can mean the transit time is practically lost, with errors of several hours (e.g. Corot-24 b and c; Alonso et al. 2014). In addition to this, extrapolating transit times from only a few data points over a limited baseline can easily introduce bias (e.g. Benneke et al. 2017). Finally, we could expect transit times to shift due to dynamical phenomena such as tidal orbital decay, apsidal precession, or from gravitational interactions with other bodies in the system (see e.g. Agol et al. 2005; Maciejewski et al. 2016; Bouma et al. 2019). These can only be understood, and mitigated for, by regularly observing targets over a long baseline. In the era of *TESS*, which is expected to find several thousand transiting planets (Sullivan et al. 2015; Barclay, Pepper & Quintana 2018), this will become increasingly difficult due to the sheer number of targets and require a coordinated effort by many groups and telescope networks to prepare for characterization by the next-generation facilities. This campaign will need data from both ground-based facilities and space-based telescopes such as *TESS*, CHEOPS, and *Twinkle*.

Ground-based follow-up will require not only a large number of telescopes but many person-hours to plan observations and process the data. Citizen astronomers, citizen science, and educational outreach offer an excellent opportunity to support future space missions. Given the brightness of the host stars of planets found by *TESS*, even modestly sized telescopes can be used to re-observe these systems, reducing the errors on their ephemerides. The ability of small ground-based telescopes to contribute to exoplanet science is well known (e.g. Kabath et al. 2019). The Next Generation Transit Survey (NGTS; Wheatley et al. 2018) has shown that sub-millimag precision is achievable by simultaneously observing the same transit with many identical small telescopes and combining data. Using such methods could expand the number of exoplanets that are observable from the ground.

Here we present a project to refine the ephemerides of eight exoplanets using a fully robotic telescope network, observations from citizen astronomers, and data from *TESS*; a significant portion of the work has been completed by high school students via the Original Research By Young Twinkle Students (ORBYTS) programme.

2 OUTREACH AND CITIZEN SCIENCE PROJECTS

The observations and analysis presented here have been achieved via engagement with several citizen science and outreach initiatives and a brief description of each of these is given below.

2.1 Original Research By Young Twinkle Students

ORBYTS is an educational programme in which secondary school pupils work on original research linked to the *Twinkle Space Mission* under the tuition of PhD students and other young scientists (McKemmish et al. 2017a; Sousa-Silva et al. 2018). The ORBYTS programme has been run since 2012 and is jointly managed by Blue Skies Space Ltd. (BSSL) and University College London (UCL). The *Twinkle Space Mission*[1] is a new, fast-track satellite designed for launch by 2024 and has been conceived for providing faster access to space-based spectroscopic data. While the satellite will also survey Solar system objects (Edwards et al. 2019a,b), a key science case for *Twinkle* is the characterization of a population of extrasolar planets via transit and eclipse spectroscopy (Edwards et al. 2019c). ORBYTS offers school pupils the chance to enrich our understanding of these new worlds by improving our knowledge of the molecules they are made of, their orbits, and their physical properties. This provides a unique opportunity for pupils to undertake cutting-edge science, which has a meaningful impact on a future space mission.

To achieve this, ORBYTS partners dynamic, passionate science researchers with secondary schools, where, through fortnightly school visits over an academic year, the researcher teaches the students undergraduate-level physics. The goal of every partnership is that school students will have the opportunity to use this new knowledge to contribute towards publishable research. Pupils get hands on experience of scientific research and work closely with young scientists. By partnering schools with relatable researchers, the programme aims to not only improve student aspirations and scientific literacy, but also help to address diversity challenges by dispelling harmful stereotypes, challenging any preconceptions about who can become a scientist. The organizers and tutors strongly believe that all school students should have the opportunity to become involved in active scientific research and to be culturally connected to space missions. Previous projects have included providing accurate molecular transition frequencies with the ExoMol group (McKemmish et al. 2017b, 2018; Chubb et al. 2018a,b; Darby-Lewis et al. 2019) as these line lists are crucial for atmospheric retrievals.

During the current project, the students selected suitable follow-up targets, scheduled observations, and analysed the observational data.

2.2 Exoplanet Transit Database

The Exoplanet Transit Database (ETD; Poddaný, Brát & Pejcha 2010) was established in 2008 and is a web-based application that is open to any exoplanet observer. The ETD is a project of the Variable Star and Exoplanet Section of the Czech Astronomical Society and the site consists of three parts, the first of which provides predictions of the upcoming transits. The second section allows for users to upload new data and the final function is the display of the observed − calculated diagrams (O − C). The ETD has hundreds of contributors and the data base contains thousands of observations. While all observations are analysed by the ETD system to produce these graphs, the data can also be downloaded. The ETD does not facilitate a ranking of planets based on their current uncertainties.

2.3 ExoWorlds Spies

ExoWorlds Spies[2] is a project that started in early 2018, aiming to monitor transiting exoplanets through long-term regular observations using small- and medium-scale telescopes. This effort is supported by citizen astronomers, the Holomon Astronomical Station, and the Telescope Live network. The project promotes the idea that research is an effort that everyone can contribute and, thus, it is open to collaborations with the public, including school and university students. To facilitate this, user-friendly data analysis tools and a dedicated website have been developed as part of the project, in order to disseminate the material to as many people as possible. The website includes audiovisual material, information on the project, data analysis tools, instructions, observational data, and graphics.

[1] http://www.twinkle-spacemission.co.uk.

[2] https://exoworldsspies.com.

All sources are online, free, and available for everyone both in English and Greek. So far, the ExoWorlds Spies data base includes approximately 60 transit observations of more than 25 different exoplanets, from both the Northern and the Southern hemisphere, including recently discovered planets with limited data available. A number of these transits are already available on the website for members of the general public, students, and citizens to analyse.

2.4 ExoClock

ExoClock has been established as part of the ground-based characterization campaign for the *Ariel* space mission. *Ariel* aims to observe 1000 exoplanets during its primary mission, characterizing their atmospheres and seeking to understand the chemical diversity of planets in our Galaxy (Tinetti et al. 2018). The *Ariel* Mission Reference Sample (MRS), the planets observed by the mission, will be selected from a large list of potential targets. The selection criterion will aim to produce a multifarious population of planets for study. However, the lack of basic knowledge such as stellar variability and the expected transit time of the system, may mean a planet is not selected for observation, potentially reducing the impact of the mission. ExoClock aims to facilitate a coordinated programme of ground-based observations to maximize the efficiency of the *Ariel* mission. The programme also aims to stimulate engagement with citizen astronomers, allowing them to contribute to an upcoming ESA mission. The site ranks the potential *Ariel* targets from Edwards et al. (2019d), prioritizing those that have a large uncertainty in their next transit time. These can then be filtered by the location of the observer and the telescope size, providing a list of exoplanet transits which would be observable in the near future. The ExoClock initiative has the explicit rule that all those who upload data for a planetary system will be included on any subsequent publications.

3 TARGET SELECTION

There are several major exoplanet catalogues from which one can compile a list of potential planets. The most widely used and comprehensive is the NASA Exoplanet Archive[3] (Akeson et al. 2013). The NASA catalogue was accessed in 2019 February and the transit error by mid-2019 (the end time of this project) was calculated for each planet. The next transit of a planet, T_c, can be calculated from

$$T_c = T_0 + n \cdot P, \tag{1}$$

where P is the period of the planet, T_0 is the last measured transit time, and n is the number of epochs since this last observation. Both T_0 and P have errors associated with their measurement and thus the error on the predicted transit time, ΔT_c , is given by

$$\Delta T_c = \sqrt{\Delta T_0^2 + (n \cdot \Delta P)^2}, \tag{2}$$

assuming no co-variance between the two parameters. There is, of course, a correlation between the fitted period and mid-time but this co-variance is generally negligible. Suitable targets were found by filtering this list to include only those with a large transit uncertainty (>10 min) or those that had not been observed for three or more years. We note that the ephemerides of many of the large, gaseous planets with significant transit uncertainties were refined by Mallonn et al. (2019) and these were excluded from the study. The choice of targets was restricted by the size of the telescopes (0.35–0.6 m, see Section 4) due to the star magnitude and transit depth but still many planets with substantial ephemeris errors were found to be observable.

[3] https://exoplanetarchive.ipac.caltech.edu.

4 DATA ACQUISITION

Table 1 contains the planets for which data were obtained and the expected transit error on 2019 July 1. Although some of the planets observed here are around relatively fainter stars, they are all potentially suitable for spectroscopic follow-up and could be observed by *Ariel* (Edwards et al. 2019d). They may also be potential targets for characterization by *Twinkle*, *JWST*, or ground-based facilities. Observations of these targets were scheduled between 2019 February and April.

4.1 Robotic ground-based telescope network

For the new observations presented here we use the Telescope Live global network of robotic telescopes.[4] Telescope Live is a web application offering end-users the possibility to purchase images obtained on-demand from a network of robotic telescopes. Telescope Live kindly provided access to their telescopes for a total of 150 h. At the time of writing, the network consists of eight telescopes distributed across three observatories: a 1-m ASA RC-1000AZ, a 0.6-m Planewave CDK24, and two 0.5-m ASA 500N located at El Sauce Observatory in Chile; a 0.7-m ProRC 700 and two 0.1-m Takahashi FSQ-106ED located at IC Astronomy in Spain; and a 0.1-m Takahashi FSQ-106ED located at Heaven's Mirror Observatory in Australia. The majority of observations were performed using a *V* filter (Luminance). Additionally, we obtained a light curve of WASP-122 b using a 1.0-m Sinistro from the Las Cumbres Observatory (LCO) network[5], thanks to the Educational Proposal FTPEPO2014A-004 led by Paul Roche.

4.2 ETD and ExoWorldSpies

For the selected planets, the ETD was searched for additional observations. The ETD provides a ranking of data quality from 1 to 5. Having removed observations with a data quality of less than 3, as well as excluding other unsuitable light curves via visual inspection, we found a total of 31 light curves from citizen astronomers: 5 of CoRoT-6 b, 21 of KPS-1 b, 3 of WASP-45 b, and 2 of WASP-122 b. All these observations were undertaken as part of the TRansiting ExoplanetS and CAndidates (TRESCA) project[6] and are summarized in Table 2. From ExoWorldSpies, we included an observation of WASP-83 b in our analysis. Additionally, the new observations taken as part of this work have been added to the ExoWorldsSpies and ExoClock data bases.

4.3 *TESS*

Having observed the Southern hemisphere, *TESS* is now surveying the Northern hemisphere and thus has observed several of the planets studied here. We searched the Mikulski Archive for Space Telescopes (MAST[7]) and found that *TESS* has observed K2-237 b, KELT-15 b, WASP-45 b, WASP-83 b, WASP-119 b, and WASP-122 b. A pipeline

[4] https://telescope.live.
[5] https://lco.global.
[6] http://var2.astro.cz/EN/tresca.
[7] http://archive.stsci.edu.

Table 1. Exoplanets for which observations were acquired and the calculated uncertainty in their transit mid-time on 2019 July 1 based on data from the NASA Exoplanet Archive.

Planet	Planet radius (R_J)	Star V mag	Uncertainty (min)	Last observed	Reference
CoRoT-6 b	1.17	13.9	2.7	2010	Fridlund et al. (2010)
KELT-15 b	1.44	11.2	15.7	2015	Rodriguez et al. (2016)
KPS-1 b	1.03	13.0	57.6	2018	Burdanov et al. (2018)
K2-237 b	1.65	11.6	13.0[a]	2018	Soto et al. (2018)
WASP-45 b	1.16	12.0	5.3	2013	Anderson et al. (2012)
WASP-83 b	1.04	12.9	11.9	2015	Hellier et al. (2015)
WASP-119 b	1.40	12.2	15.7	2016	Maxted et al. (2016)
WASP-122 b	1.74	11.0	4.9[b]	2016	Turner et al. (2016)

[a]The independent discovery paper (Smith et al. 2018) suggests an uncertainty of 3.8 min.
[b]The independent discovery paper (Rodriguez et al. 2016) suggests an uncertainty of 3.4 min.

was built to find, acquire, reduce, and analyse the data. For a given target, the code searches MAST and returns all the data collected on the host star from various observatories. The list is filtered to see if *TESS* has observed the star and, if so, the presearch data conditioning (PDC) light curve, which has had non-astrophysical variability removed and 'bad data' eliminated through the methods outlined in the *TESS* guide,[8] is downloaded. The data product is a time-series for each sector (∼27 d) with a cadence of two min. After excluding the poor data, we recovered 7 K2-237 b transits, 12 for KELT-15 b, 8 for WASP-45 b, 4 of WASP-83 b along with 37 for WASP-119 b and 13 of WASP-122 b.

5 DATA REDUCTION AND ANALYSIS

The Telescope Live network automatically gathers calibration frames and provides the data in a reduced format (though the raw and calibration frames can also be downloaded). These frames were analysed using the HOlomon Photometric Software (HOPS), which aligns the frames and normalizes the flux of the target star by using selected comparison stars. This software is open-source and available on GITHUB.[9]

The photometric light curves from all sources were fitted using PYLIGHTCURVE (Tsiaras et al. 2016), another code that is publicly available.[10] Initially, fitted parameters were the orbital semi-major axis scaled by the stellar radius (a/R_*), the orbital inclination (i), the planet-to-star radius ratio (R_p/R_*), the mid-point of the transit (T), and the orbital period (P). In each case, the Markov chain Monte Carlo (MCMC) was run with 100 000 iterations, a burn of 30 000, and 200 walkers. The limb-darkening coefficients were fixed to theoretical values from Claret, Hauschildt & Witte (2012, 2013) according to the stellar parameters obtained from the planet discovery papers and the initial ephemerides were those listed in Table 3. Previous analyses show that the trends in ground-based light curves can be approximated with simple functions of only very few free parameters, for example, low-order polynomials over time (e.g. Southworth 2011; Maciejewski et al. 2016; Mackebrandt et al. 2017; Mallonn et al. 2019). Hence we detrended all ground-based light curves using a simple second-order polynomial. We then removed all data points with residuals greater than 3σ from the best-fitting model. For *TESS* data, we used the flatten function from WOTAN (Hippke et al. 2019), an open-source PYTHON suite developed for comprehensive time-series detrending of Exoplanet Transit Survey data.[11]

Next, we fitted each light curve individually with a/R_*, i and R_p/R_* allowed to vary within 1σ of the values from the literature (or the new values computed here) while T was fitted with bounds of 3σ. For targets that had been observed by *TESS*, we refined the planet transit parameters (R_p/R_*, i, a/R_*) and these are provided in Tables 4, 5 & 6. The uncertainties on each fitted mid-time are obtained from the posterior distributions of the MCMC chains. We convert all our mid-times into $\mathrm{BJD_{TDB}}$ using the tool from Eastman, Siverd & Gaudi (2010). Having fit the mid-transit time for all the data, we use a weighted least-squares fit to obtain a linear period for the data analysed in this work and any previous mid-times from the literature (also converted into $\mathrm{BJD_{TDB}}$). We varied the reference transit time, T_0, and report the value that minimized the co-variance between T_0 and P.

Finally, we used the literature ephemerides from Table 3 to compute 'observed minus calculated' residuals for all transit times and used our refined ephemerides to predict the uncertainty on the transit times when *Ariel* is launched in 2028.

6 RESULTS

Our analysis shows significant drifts in the transit times of all planets studied here, with only one planet (KPS-1 b) having observed transits within the 1σ errors on the expected time as shown in Fig. 1. Even in this case, the observed transit was considerably offset from that predicted. K2-237 b, KELT-15 b, WASP-45 b, WASP-83 b, WASP-119 b, and WASP-122 b were observed by *TESS* in the first year of operations and we demonstrate the great potential the mission has for refining orbital parameters. The capability of *TESS* to provide accurate updated ephemerides for bright, short-period planets has previously been shown in Bouma et al. (2019). The fitted light curves from all sources are shown in Figs 1–8.

As the primary two-year mission covers almost the entire sky, the ephemerides of many of the known planets could be updated once the data are released. For short-period planets, *TESS* data give multiple high-precision, complete transits allowing the uncertainty on both the period and T_0 of these planets to be reduced. A summary of the findings for each planet is given as follows:

CoRoT-6 b: Raetz et al. (2019) found that CoRoT planets seemed to have slightly underestimated uncertainties in their ephemerides and our analysis of CoRoT-6 b agrees with their findings. The last transit of CoRoT-6 b was found to be 23 min after the calculated

[8]https://spacetelescope.github.io/notebooks/notebooks/MAST/TESS/beginner_tour_lc_tp/beginner_tour_lc_tp.html.
[9]https://github.com/HolomonAstronomicalStation/hops.
[10]https://github.com/ucl-exoplanets/pylightcurve.
[11]https://github.com/hippke/wotan.

Table 2. General information about the observations conducted and analysed in this work.

Planet	Date	Telescope	Filter	Exposure time (s)	Mid-time (BJD)	Mid-time error	Epoch	Label
	2020 Jul 9	ETD, Sauer	Clear	90	2455386.52167	0.000 85	63	G1
	2020 Jul 17	ETD, Sauer	Clear	90	2455395.40632	0.000 74	64	G2
CoRoT-6 b	2015 Jun 17	ETD, Molina	Clear	300	2457190.50697	0.006 98	266	G3
	2018 Jul 19	ETD, Kang	*R*	300	2458319.10958	0.001 02	393	G4
	2019 Jun 22	ETD, Evans	Clear	300	2458656.80291	0.002 42	431	G5
K2-237 b	Apr 16	El Sauce	*V*	30	2458589.73380	0.000 61	370	G1
		TESS S12	*I*	120	2458631.16350	0.000 95	389	T1
					2458633.34306	0.000 77	390	T2
	2019 May 26				2458635.52308	0.000 78	391	T3
	till				2458637.70413	0.000 95	392	T4
	Jun 18				2458646.42401	0.000 89	396	T5
					2458648.60616	0.000 97	397	T6
					2458650.78837	0.000 90	398	T7
		TESS S7,9	*I*	120	2458494.13536	0.000 68	−10	T1
					2458497.46521	0.000 61	−9	T2
					2458500.79344	0.000 62	−8	T3
					2458507.45364	0.000 67	−6	T4
	2019 Jan 8				2458510.78149	0.000 68	−5	T5
KELT-15 b	till				2458514.11222	0.000 66	−4	T6
	Mar 27				2458547.40593	0.000 73	6	T7
					2458550.73620	0.000 77	7	T8
					2458554.06598	0.000 72	8	T9
					2458560.72358	0.000 78	10	T10
					2458564.05458	0.000 74	11	T11
					2458567.38262	0.000 75	12	T12
	2019 Feb 19	Warrumbungle	*V*	120	2458534.08713	0.0024	2	G1
	2019 Mar 21	Warrumbungle	*V*	120	2458564.05478	0.003 58	11	G2
	2019 Mar 12	ETD, Jongen	Clear	120	2458554.34979	0.000 64	−10	G1
	2019 Mar 22	ETD, Wunsche	*V*	120	2458564.58226	0.000 96	−4	G2
	2019 Mar 22	ETD, Wunsche	Clear	120	2458564.58759	0.001 64	−4	G3
	2019 Mar 22	ETD, Raetz	Clear	60	2458564.58547	0.000 90	−4	G4
	2019 Mar 22	ETD, Jongen	Clear	120	2458564.58697	0.000 93	−4	G5
	2019 Mar 22	ETD, Guerra	CBB	120	2458564.58415	0.000 60	−4	G6
	2019 Mar 29	ETD, Wunsche	Clear	120	2458571.40954	0.001 82	0	G7
	2019 Mar 29	ETD, Jongen	Clear	120	2458571.41164	0.000 47	0	G8
	2019 Mar 29	ETD, Friedli/Kropf	*V*	60	2458571.40894	0.000 25	0	G9
	2019 Mar 29	ETD, Watkins	*R*	30	2458571.41121	0.000 65	0	G10
KPS-1 b	2019 Mar 29	ETD, Guerra	*I*	180	2458571.41002	0.000 98	0	G11
	2019 Apr 20	ETD, Wunsche	Clear	120	2458593.59136	0.001 47	13	G12
	2019 Apr 20	ETD, Jongen	Clear	120	2458593.59541	0.001 13	13	G13
	2019 May 2	ETD, Raetz	Clear	120	2458605.53684	0.000 99	20	G14
	2019 May 14	ETD, Bretton	*I*	120	2458617.47815	0.000 85	27	G15
	2019 May 14	ETD, Guerra	*V*	180	2458617.48126	0.000 66	27	G16
	2019 May 14	ETD, Raetz	Clear	120	2458617.48309	0.000 79	27	G17
	2019 May 14	ETD, Bosch	*V*	200	2458617.48291	0.000 35	27	G18
	2019 May 14	ETD, Watkins	*V*	30	2458617.48255	0.001 62	27	G19
	2019 May 31	ETD, Bretton	Clear	120	2458634.54617	0.000 26	37	G20
	2019 May 31	ETD, Jongen	Clear	120	2458634.54662	0.000 50	37	G21
	2011 Aug 15	ETD, Evans	Clear	60	2455782.01348	0.000 97	−550	G1
	2012 Jul 16	ETD, Sauer	*R*	60	2456119.62831	0.000 97	−442	G2
	2016 Dec 27	ETD, Lajus	*R*	10	2457660.78567	0.000 56	51	G3
		TESS S2	*I*	120	2458354.77330	0.000 93	273	T1
WASP-45 b					2458357.89881	0.000 85	274	T2
					2458361.02613	0.000 79	275	T3
	2018 Aug 23				2458364.15241	0.001 10	276	T4
	till				2458370.40257	0.000 89	278	T5
	2019 Sep 20				2458373.52974	0.000 96	279	T6
					2458376.65588	0.000 77	280	T7
					2458379.78198	0.000 88	281	T8

Table 2 – *continued*

Planet	Date	Telescope	Filter	Exposure time (s)	Mid-time (BJD)	Mid-time error	Epoch	Label
	2019 Apr 2	El Sauce	*R*	120	2458205.73765	0.000 83	213	G1
WASP-83 b	2019 Mar 28 till Apr 22	*TESS* S10	*I*	120	2458573.61364	0.000 90	287	T1
					2458578.58484	0.000 95	288	T2
					2458588.52739	0.001 14	290	T3
					2458593.49776	0.000 94	291	T4
WASP-119 b	2018 Jul 27 till 2019 May 18	*TESS* S1-4,7,11	*I*	120	2458327.40896	0.000 64	−33	T1
					2458329.90921	0.000 63	−32	T2
					2458332.40913	0.000 69	−31	T3
					2458334.90914	0.000 59	−30	T4
					2458337.40888	0.000 71	−29	T5
					2458342.40948	0.000 63	−27	T6
					2458344.90830	0.000 62	−26	T7
					2458347.40851	0.001 47	−25	T8
					2458349.90839	0.000 63	−24	T9
					2458352.40769	0.000 61	−23	T10
					2458354.90856	0.000 80	−22	T11
					2458357.40699	0.000 74	−21	T12
					2458359.90699	0.000 71	−20	T13
					2458362.40801	0.000 70	−19	T14
					2458364.90547	0.000 82	−18	T15
					2458369.90681	0.000 67	−16	T16
					2458372.40655	0.000 79	−15	T17
					2458374.90585	0.000 74	−14	T18
					2458377.40605	0.000 64	−13	T19
					2458379.90440	0.000 71	−12	T20
					2458387.40490	0.000 71	−9	T21
					2458389.90515	0.000 68	−8	T22
					2458392.40410	0.000 66	−7	T23
					2458394.90473	0.000 87	−6	T24
					2458397.40311	0.000 64	−5	T25
					2458399.90351	0.000 64	−4	T26
					2458402.40275	0.000 58	−3	T27
					2458404.90377	0.000 59	−2	T28
					2458412.40318	0.000 71	1	T29
					2458414.90327	0.000 70	2	T30
					2458417.40304	0.000 64	3	T31
					2458422.40234	0.000 68	4	T32
					2458424.90216	0.000 60	6	T33
					2458427.40244	0.000 66	7	T34
					2458429.90269	0.000 63	8	T35
					2458432.40216	0.000 62	9	T36
					2458434.90223	0.000 69	10	T37
					2458492.39645	0.001 17	33	T38
					2458494.89668	0.001 29	34	T39
					2458497.39677	0.001 23	35	T40
					2458499.89584	0.001 28	36	T41
					2458502.39712	0.001 12	37	T42
					2458504.89546	0.001 27	38	T43
					2458507.39514	0.001 30	39	T44
					2458509.89502	0.001 23	40	T45
					2458512.39476	0.001 22	41	T46
					2458514.89459	0.001 30	42	T47
					2458602.38802	0.000 85	77	T48
					2458604.88824	0.000 88	78	T49
					2458607.38852	0.000 76	79	T50
					2458614.88619	0.000 89	82	T51
					2458617.38771	0.000 84	83	T52
					2458619.88570	0.000 83	84	T53
					2458622.38559	0.000 76	85	T54
	2019 Mar 7	Warrumbungle	*V*	60	2458549.89284	0.00596	56	G1

Table 2 – *continued*

Planet	Date	Telescope	Filter	Exposure time (s)	Mid-time (BJD)	Mid-time error	Epoch	Label
	2017 Jan 18	ETD, Evans	*R*	75	2457771.62839	0.000 35	−59	G1
	2017 Jan 30	ETD, Evans	*R*	80	2457783.59845	0.000 44	−52	G2
	2019 Mar 2	LCO	*V*	5	2458544.57156	0.000 61	393	G3
WASP-122 b	2019 Jan 8 till Feb 1	*TESS* S7	*I*	120	2458493.27195	0.000 52	363	T1
					2458494.98245	0.000 56	364	T2
					2458496.69209	0.000 56	365	T3
					2458498.40213	0.000 55	366	T4
					2458500.11221	0.000 56	367	T5
					2458501.82282	0.000 54	368	T6
					2458505.24207	0.000 55	370	T7
					2458506.95200	0.000 55	371	T8
					2458508.66246	0.000 54	372	T9
					2458510.37276	0.000 53	373	T10
					2458512.08277	0.000 58	374	T11
					2458513.79187	0.000 60	375	T12
					2458515.50265	0.000 56	376	T13

Note. The label corresponds to that given in Figs 2 and 3.

Table 3. Summary of literature ephemeris data used here.

Planet	Mid-time (BJD_{TDB})	Period (d)	Reference
CoRoT-6 b	2454595.6144 ± 0.0002	8.886 593 ± 0.000 004	Fridlund et al. (2010)
K2-237 b	2457684.8101 ± 0.0001	2.180 56 ± 0.000 02	Soto et al. (2018)
KELT-15 b	$2457029.1663^{+0.0078}_{-0.0073}$	3.329 441 ± 0.000 016	Rodriguez et al. (2016)
KPS-1 b	$2457508.37019^{+0.0079}_{-0.0078}$	1.706 291 ± 0.000 059	Burdanov et al. (2018)
WASP-45 b	2455441.269995 ± 0.00058	3.126 0876 ± 0.000 0035	Anderson et al. (2012)
WASP-83 b	2455928.886085 ± 0.0004	4.971 252 ± 0.000 015	Hellier et al. (2015)
WASP-119 b	2456537.547779 ± 0.002	2.499 79 ± 0.000 01	Maxted et al. (2016)
WASP-122 b	2456665.224782 ± 0.00021	$1.710\,0566^{+0.000\,0032}_{-0.000\,0026}$	Turner et al. (2016)

Table 4. Summary of updated system parameters for CoRoT-6 b, K2-237 b, and KELT-15 b.

Parameter	Units	CoRoT-6 b	K2-237 b	KELT-15 b
R_*	Star radius ($R_\odot$)	1.025 ± 0.026^a	$1.43^{+0.06\,b}_{-0.07}$	$1.481^{+0.091\,c}_{-0.041}$
M_*	Star mass ($M_\odot$)	1.05 ± 0.05	$1.28^{+0.03\,b}_{-0.04}$	$1.181^{+0.051\,c}_{-0.050}$
T_{eff}	Star effective temperature (K)	6090 ± 70^a	6257 ± 100^b	$6003^{+56\,c}_{-52}$
Fe/H	Star metallicity	-0.2 ± 0.1^a	0.14 ± 0.05^b	0.047 ± 0.032^c
$\log(g_*)$	Star surface gravity (cgs)	4.43 ± 0.1^a	4.24 ± 0.1^b	$4.168^{+0.019\,c}_{-0.044}$
ρ_*	Star density ($\rho_\odot$)	1.31 ± 0.09^a	$0.144^{+0.017\,b}_{-0.014}$	$0.514^{+0.034\,c}_{-0.076}$
R_P	Planet radius (R_J)	1.166 ± 0.035^a	$1.6944^{+0.0118}_{-0.0103}$	$1.4745^{+0.0033}_{-0.0415}$
R_P	Planet radius ($R_\oplus$)	13.068 ± 0.392^a	$18.5935^{+0.1298}_{-0.1136}$	$16.180\,20^{+0.003\,64}_{-0.455\,55}$
R_P/R_*	Planet radius in stellar radii	0.1198 ± 0.0036^a	$0.12342^{+0.000\,86}_{-0.000\,75}$	$0.1000^{+0.000\,22}_{-0.002\,81}$
δ	Transit depth	0.17 ± 0.0008^a	$0.01523^{+0.000\,21}_{-0.000\,19}$	$0.0100^{+0.000\,05}_{-0.000\,56}$
M_P	Planet mass (M_J)	2.96 ± 0.34^a	1.6 ± 0.11^b	$0.910^{+0.210\,c}_{-0.220}$
M_P	Planet mass ($M_\oplus$)	940.74 ± 108.06^a	509 ± 35^b	$289^{+67\,c}_{-70}$
P	Period (d)	8.886 621 ± 0.000 0063	2.180 5358 ± 0.000 0010	3.329 468 ± 0.000 012
T_0	Transit mid-time (BJD_{TDB})	2454826.66625 ± 0.00054	2457782.93422 ± 0.00014	2458527.42971 ± 0.00017
a	Semi-major axis (AU)	0.0855 ± 0.0015^a	$0.036\,02^{+0.000\,23}_{-0.000\,42}$	$0.047\,78^{+0.000\,22}_{-0.0082}$
a/R_*	Semi-major axis in stellar radii	17.94 ± 0.33^a	$5.6138^{+0.0364}_{-0.0655}$	$6.940^{+0.032}_{-0.118}$
i	Inclination (°)	89.07 ± 0.3^a	$84.888^{+0.024}_{-0.264}$	$88.339^{+0.169}_{-0.052}$
b	Impact parameter	0.291 ± 0.091^a	0.500 ± 0.005 83	0.1946 ± 0.0048
e	Eccentricity	Fixed to zero	Fixed to zero	Fixed to zero

[a]Fridlund et al. (2010). [b]Soto et al. (2018). [c]Rodriguez et al. (2016).

transit time despite the predicted uncertainty being less than 3 min. The new observations help reduce the uncertainty on the transit time, but we note there is not currently enough data to accurately constrain the period.

Table 5. Summary of updated system parameters for KPS-1 b, WASP-45 b, and WASP-83 b.

Parameter	Units	KPS-1 b	WASP-45 b	WASP-83 b
R_*	Star radius ($R_\odot$)	$0.907\ ^{+0.086}_{-0.082}$[a]	0.945 ± 0.087[a]	$1.05^{+0.06}_{-0.04}$[c]
M_*	Star mass ($M_\odot$)	$0.892\ ^{+0.090}_{-0.100}$[b]	0.909 ± 0.060[b]	1.11 ± 0.09[d]
$T_{\rm eff}$	Star effective temperature (K)	5165 ± 90[a]	5140 ± 200[b]	5510 ± 110[d]
Fe/H	Star metallicity	0.22 ± 0.13[a]	0.43 ± 0.06[c]	0.29 ± 0.12[d]
$\log(g_*)$	Star surface gravity (cgs)	4.47 ± 0.06[a]	4.43 ± 0.18[c]	$4.44\ ^{+0.02}_{-0.04}$[c]
ρ_*	Star density ($\rho_\odot$)	$1.68\ ^{+0.41}_{-0.32}$[a]	1.08 ± 0.25[c]	$1.40\ ^{+0.10}_{-0.18}$[c]
$R_{\rm P}$	Planet radius (R_J)	$1.03\ ^{+0.13}_{-0.12}$[a]	$1.079\ ^{+0.047}_{-0.016}$	$1.039\ ^{+0.012}_{-0.008}$
$R_{\rm P}$	Planet radius (R_E)	$11.5\ ^{+1.5}_{-1.3}$[a]	$11.849^{+0.519}_{-0.173}$	$11.402\ ^{+0.129}_{-0.086}$
$R_{\rm P}/R_*$	Planet radius in stellar radii	$0.1143\ ^{+0.0037}_{-0.0034}$[a]	$0.1149^{+0.0050}_{-0.0017}$	$0.09947^{+0.00113}_{-0.00075}$
δ	Transit depth	$0.013\,06\ ^{+0.001\,65}_{-0.001\,70}$[a]	$0.013\,19\ ^{+0.001\,16}_{-0.000\,39}$	$0.009\,895\ ^{+0.002\,24}_{-0.000\,15}$
$M_{\rm P}$	Planet mass (M_J)	$1.090\ ^{+0.086}_{-0.087}$[a]	1.007 ± 0.053[b]	0.30 ± 0.03[d]
$M_{\rm P}$	Planet mass ($M_\oplus$)	$346.4\ ^{+27.3}_{-27.7}$[a]	320.0421 ± 16.844[b]	95 ± 10[d]
P	Period (d)	$1.706\,3270 \pm 0.000\,0036$	$3.126\,076\,37 \pm 0.000\,000\,60$	$4.971\,291\,75 \pm 0.000\,000\,51$
T_0	Transit mid-time (BJD$_{\rm TDB}$)	$2458571.41092 \pm 0.00035$	$2457501.35468 \pm 0.00022$	$2457146.85256 \pm 0.00013$
a	Semi-major axis (AU)	0.0269 ± 0.001[a]	$0.042\,95\ ^{+0.000\,48}_{-0.001\,61}$	$0.0592\ ^{+0.0019}_{-0.0009}$
a/R_*	Semi-major axis in stellar radii	$6.38^{+0.77}_{-0.72}$[a]	$9.78^{+0.11}_{-0.36}$	$12.1\,3^{+0.39}_{-0.19}$
i	Inclination (°)	$83.20^{+0.88}_{-0.90}$[a]	$84.98^{+0.03}_{-0.31}$	$88.91^{+0.50}_{-0.43}$
b	Impact parameter	0.754 ± 0.049[a]	0.855 ± 0.032	0.28 ± 0.007
e	Eccentricity	Fixed to zero	Fixed to zero	Fixed to zero

[a]Burdanov et al. (2018). [b]Anderson et al. (2012). [c]Mortier et al. (2013). [d]Hellier et al. (2015).

Table 6. Summary of updated system parameters for WASP-119 b and WASP-122 b.

Parameter	Units	WASP-119 b	WASP-122 b
R_*	Star radius ($R_\odot$)	1.2 ± 0.1[a]	1.52 ± 0.03[b]
M_*	Star mass ($M_\odot$)	1.02 ± 0.06[a]	1.239 ± 0.039[b]
$T_{\rm eff}$	Star effective temperature (K)	5650 ± 100[a]	5720 ± 130[b]
Fe/H	Star metallicity	0.14 ± 0.10[a]	$0.32\pm$[b]
$\log(g_*)$	Star surface gravity (cgs)	4.26 ± 0.08[a]	4.166 ± 0.016[b]
ρ_*	Star density ($\rho_\odot$)	0.76 ± 0.25[a]	0.495 ± 0.025[b]
$R_{\rm P}$	Planet radius (R_J)	$1.3542\ ^{+0.0039}_{-0.0023}$	$1.712\ ^{+0.009}_{-0.006}$
$R_{\rm P}$	Planet radius (R_E)	$14.860\ ^{+0.043}_{-0.0255}$	$18.785\ ^{+0.102}_{-0.068}$
$R_{\rm P}/R_*$	Planet radius in stellar radii	$0.113\,44\ ^{+0.000\,32}_{-0.000\,19}$	$0.1132\ ^{+0.0006}_{-0.0004}$
δ	Transit depth	$0.0128\,68\ ^{+0.000\,074}_{-0.000\,044}$	$0.0128\,15\ ^{+0.000\,139}_{-0.000\,093}$
$M_{\rm P}$	Planet mass (M_J)	1.23 ± 0.08[a]	1.284 ± 0.032[b]
$M_{\rm P}$	Planet mass ($M_\oplus$)	391 ± 25[a]	408.1 ± 10.2[b]
P	Period (d)	$2.499\,8052 \pm 0.000\,0017$	$1.710\,053\,44 \pm 0.000\,000\,32$
T_0	Transit mid-time (BJD$_{\rm TDB}$)	$2458409.903247 \pm 0.000086$	$2457872.52231 \pm 0.00015$
a	Semi-major axis (AU)	$0.038\,51\ ^{+0.000\,08}_{-0.000\,21}$	$0.030\,24\ ^{+0.000\,07}_{-0.000\,19}$
a/R_*	Semi-major axis in stellar radii	$6.902\ ^{+0.014}_{-0.037}$	$4.279^{+0.01}_{-0.027}$
i	Inclination (°)	$86.99\ ^{+0.01}_{-0.11}$	$78.595\ ^{+0.009}_{-0.010}$
b	Impact parameter	0.362 ± 0.002	0.846 ± 0.005
e	Eccentricity	Fixed to zero	Fixed to zero

[a]Maxted et al. (2016). [b]Turner et al. (2016).

K2-237 b: There are two independent discovery papers for K2-237 b. Using the ephemeris data from Soto et al. (2018), one could expect an uncertainty of 13 min in the transit mid-time, while Smith et al. (2018) claim a greater precision on the period and thus predicts an uncertainty of 3 min. In reality, we discover a shift of nearly 15 min and find our data to have a closer fit to the ephemerides of Soto et al. (2018). However, given the short period of the planet (∼2.18 d), over 400 orbits have occurred since the discovery. The difference is therefore equivalent to an error in the period of ∼1.5 s, compared to a claimed uncertainty in the period of 0.5 s), and shows how slight errors in the accuracy of exoplanet ephemerides can lead to significant deviations from the expected transit time, highlighting the benefit of following up targets on a regular basis.

KELT-15 b: This hot Jupiter had not been re-observed with transit photometry since its discovery, meaning the uncertainty in its transit time had risen to nearly 16 min. In the four years since, several hundred orbits had occurred and a 20-min deviation from the expected transit time was found.

KPS-1 b: The newly observed transits for this planet were the only ones to fall within the 1σ errors in our sample. However, a deviation from the expected transit time of over 30 min was found, which

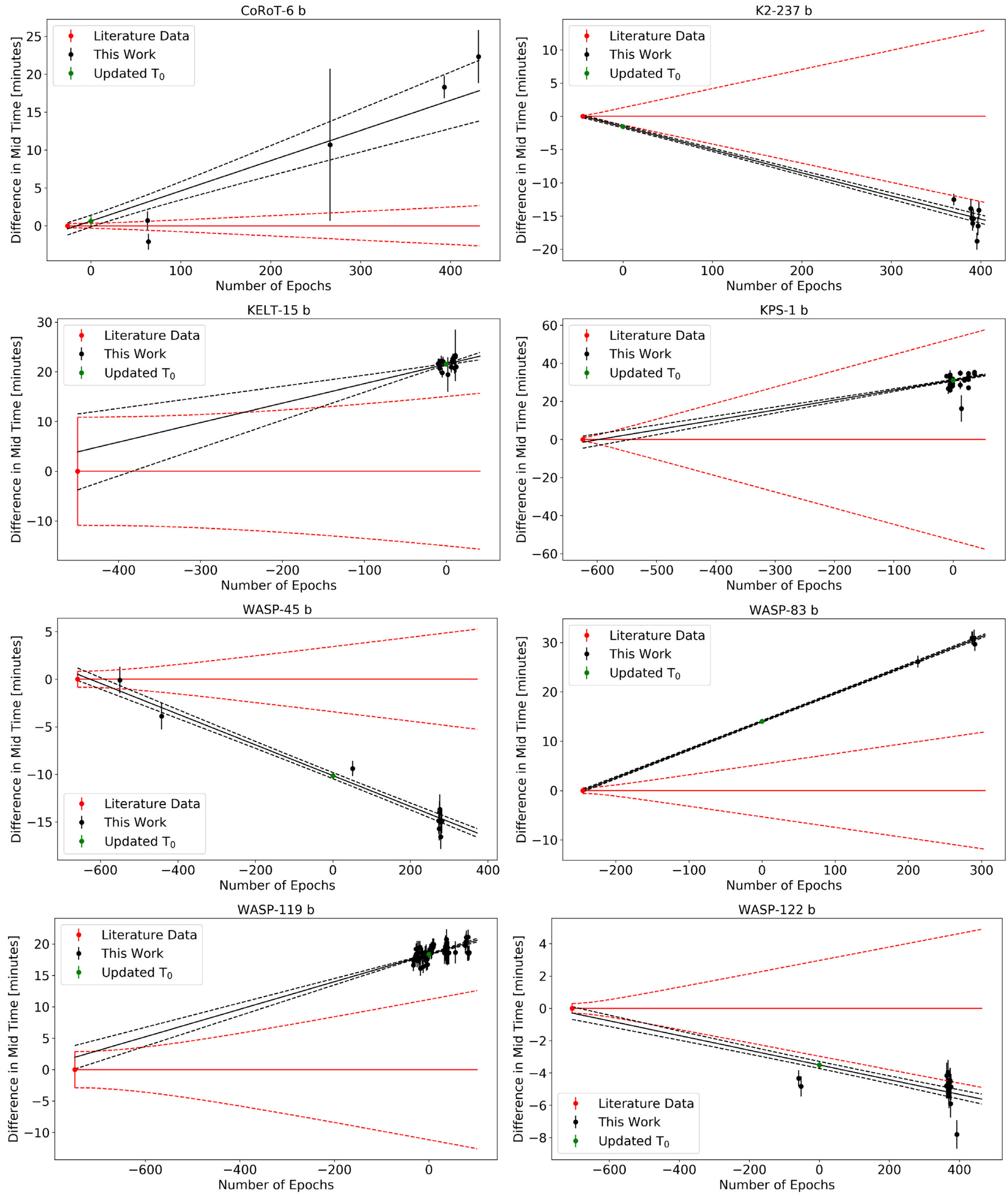

Figure 1. Observed minus calculated mid-transit times for all planet studied here. Transit mid-time measurements from this work are shown in black, while literature T_0 values included in our calculation are in red. The green data point shows the updated T_0 reported. The black line denotes the new ephemerides of this work with the dashed lines showing the associated 1σ uncertainties. For comparison, the previous literature ephemerides are given in red.

is still a substantial residual. The uncertainty on the transit time of KPS-1 b is predicted to be less than 10 min until after the launch of *Ariel* in 2028.

WASP-45 b: The predicted uncertainty on WASP-45 b was around 5 min but had not been re-observed for several years. The O − C plot from ETD showed a slight divergence from that expected but it was

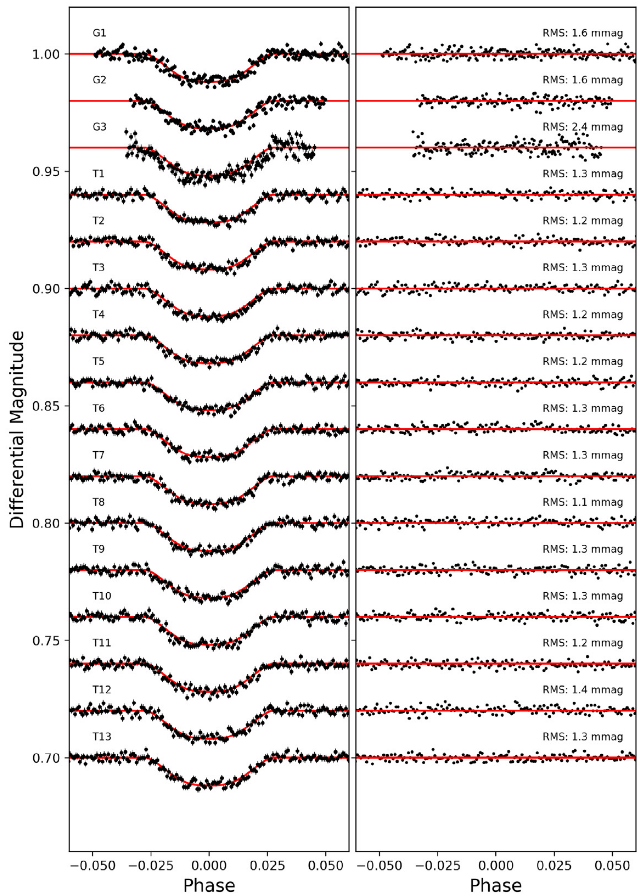

Figure 2. All the observations of WASP-122 b used in this work.

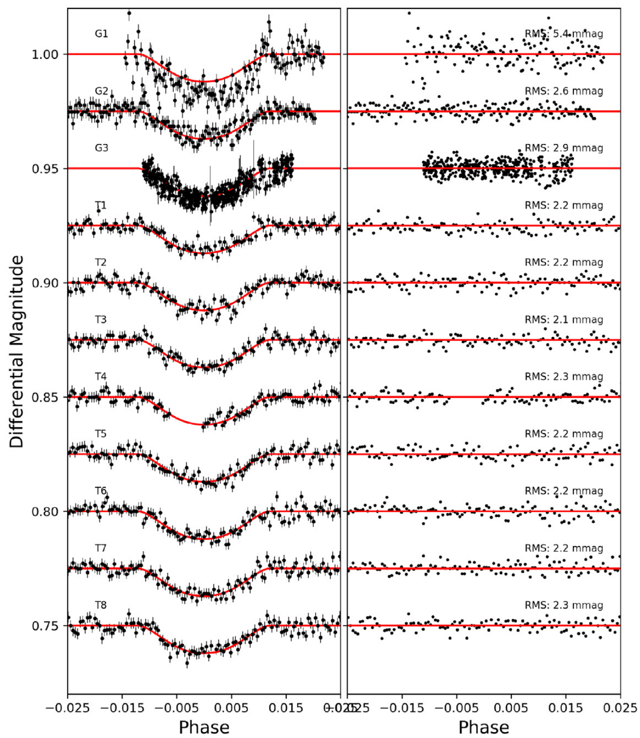

Figure 3. All the observations of WASP-45 b used in this work.

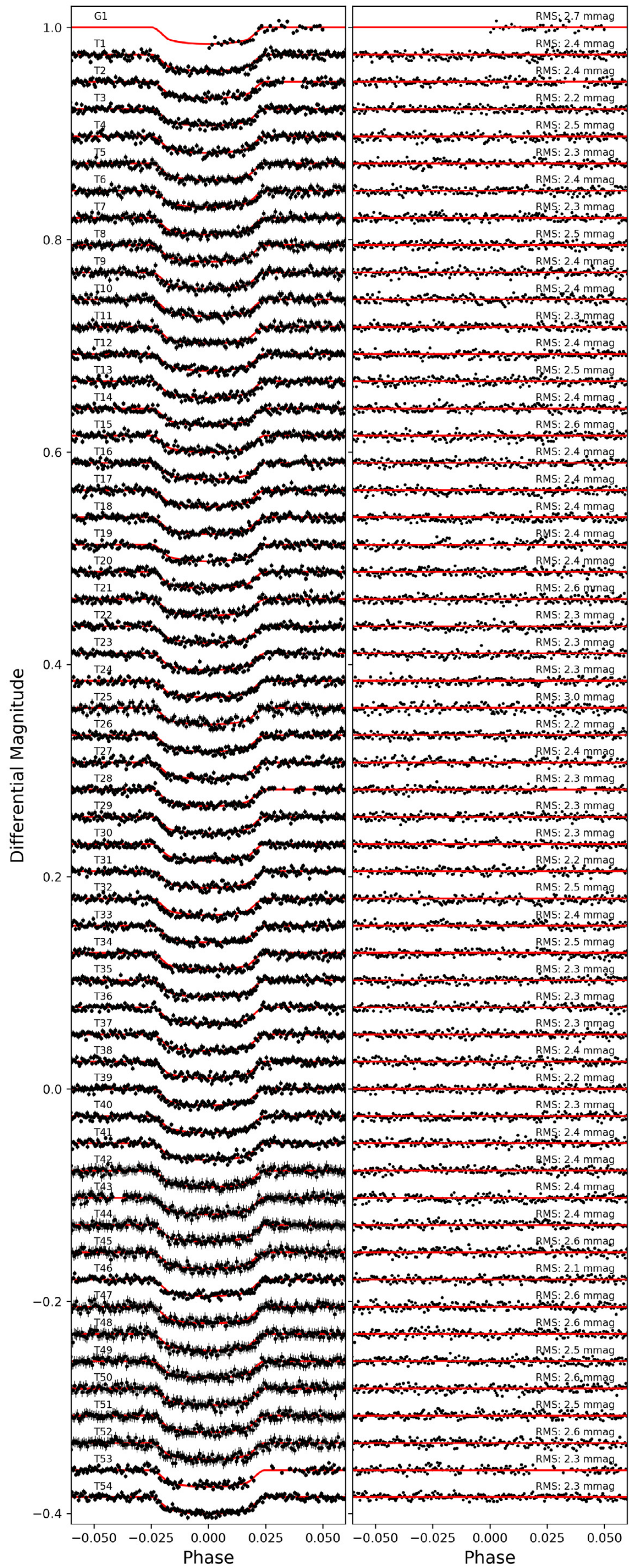

Figure 4. All the observations of WASP-119 b used in this work.

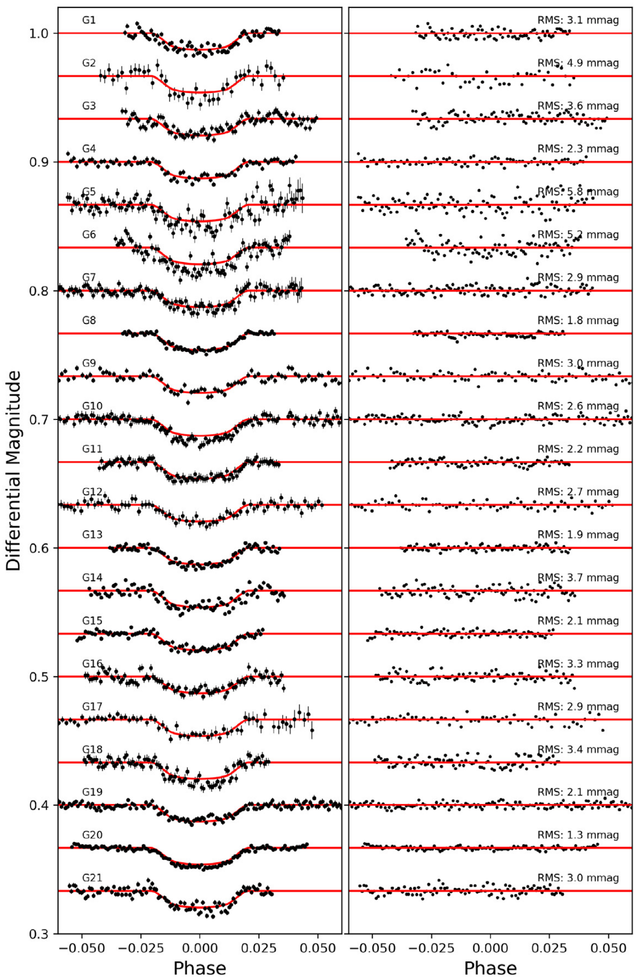

Figure 5. All the observations of KPS-1 b used in this work.

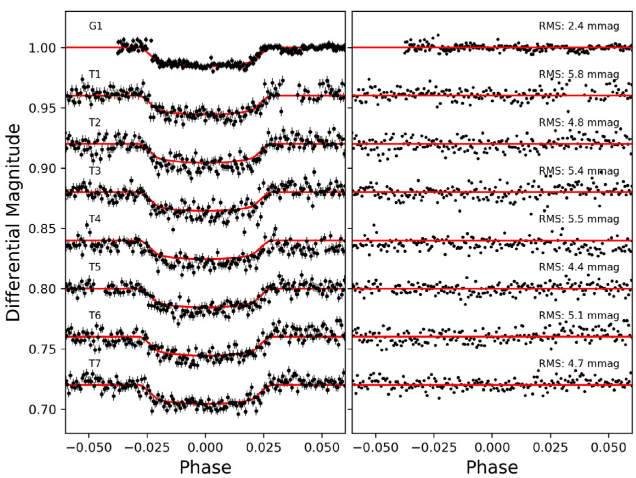

Figure 6. The observation of K2-237 b used in this work.

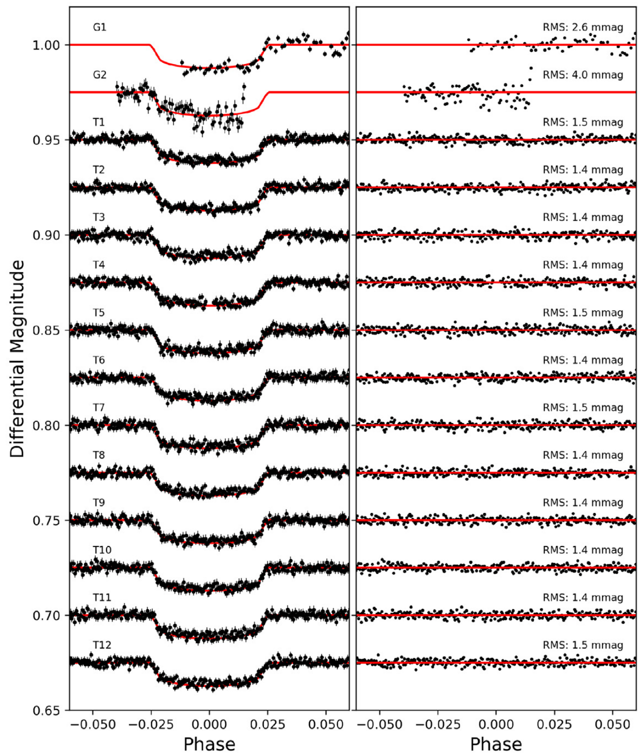

Figure 7. All the observations of KELT-15 b used in this work.

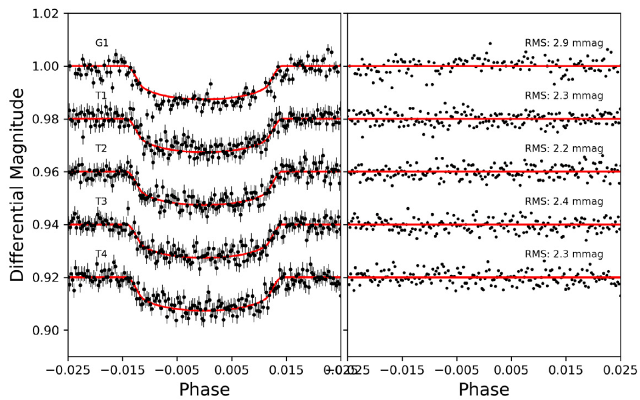

Figure 8. All the observations of WASP-83 b used in this work.

not until the *TESS* data were analysed the full extent became clear with the transit arriving 15 min early.

WASP-83 b: For WASP-83 b, the newly observed transits occurred ∼30 min after the expected time, well outside the 1σ error of ∼12 min. Having not been observed since 2015, 300 orbits had passed. The literature orbital period differs by only 6 s from the updated value reported here, again highlighting the need for consistent follow-up.

WASP-119 b: With a reported discovery of ephemerides in 2013 and an uncertainty of over 10 min, WASP-119 b was an obvious choice for follow-up. The combination of *TESS* data and a ground-based observation uncovered a drift of nearly 20 min over the 700 orbits since discovery.

WASP-122 b: Also known as KELT-14 b, this planet has two independent discovery papers (Rodriguez et al. 2016; Turner et al. 2016). These papers gave uncertainties of 3.4 and 4.9 min on the current transit mid-time and the planet had not been re-observed since its discovery. Our observations found the transits of WASP-122 b to be occurring around 5 min early, just outside the 1σ errors. We find our data have a better fit to the period from Turner et al. (2016).

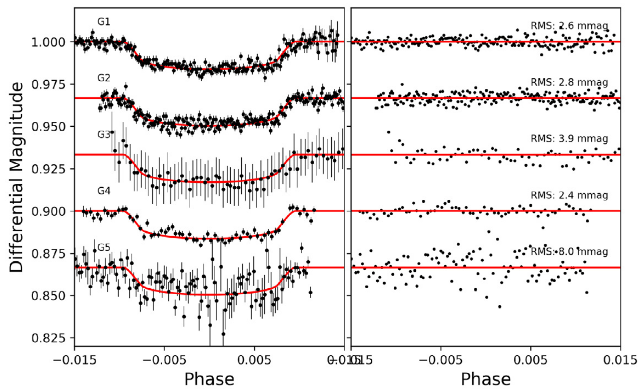

Figure 9. The observation of CoRoT-6 b used in this work.

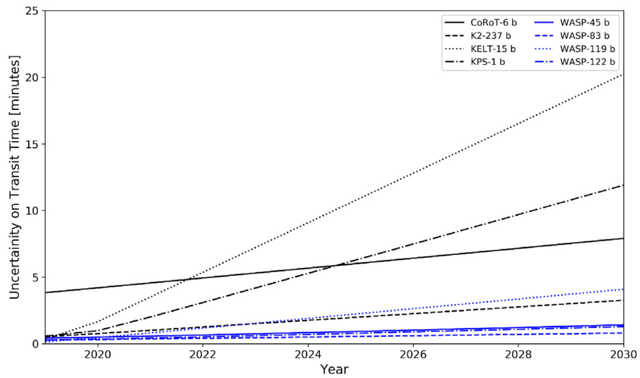

Figure 10. Projected uncertainties in the transit time of the planets studied here.

Hence, we detect significant variations in the observed transit time from the expected for most of the planets studied here. An overconfidence in the predicted transit time is a known issue and analysis of measured-to-predicted timing deviations of 21 exoplanets by Mallonn et al. (2019) indicated a trend of slightly underestimated uncertainties in the ephemerides, while Raetz et al. (2019) made a similar finding for CoRoT planets. Mallonn et al. (2019) found an average deviation of 1.4σ while here we find a 2.2σ divergence. We note that this is largely driven by CoRoT-6 b, which was observed to transit 7.7σ from the expected time, and removing this planet reduces the average deviation to 1.5σ.

Here our analysis claims sub-second uncertainties on the periods of K2-237 b, WASP-45 b, WASP-83 b, WASP-119 b, and WASP-122 b, which should keep the uncertainty on the transit times of these planets to below 15 min until well after the launch of *Ariel* in 2028 (see Figs 9 and 10). Nevertheless, we would advocate further follow-up of these planets, the others studied here and further planets with seemingly accurate ephemeris data to ensure errors are not underestimated. A cause of this can be the short baseline over which the period of the planet is determined when it is first discovered. When extrapolated over long times periods, even slight inaccuracies in the fitted period can cause significant deviations. Other sources of larger than expected uncertainties can be due to underestimated systematics in the data, stellar activity, tidal effects, or transit timing variations (TTVs) due to other bodies in the system. Additionally, while the co-variance between T_0 and the period is minimised during fitting, it is non-zero. These effects can only be mitigated for by regularly observing transits over a long time period, and to achieve this, a well-organized ground- and space-based campaign is required.

In any case, we emphasize that even in the event of the ephemerides being affected by astrophysical disturbances, our new ephemerides present the best available basis for future follow-up studies.

7 DISCUSSION

The next generation of telescopes (*JWST*, *Ariel*, ELT, etc.) will require rigorous scheduling to minimize overheads and maximize science outputs. This means interesting science targets could see their observing priority degraded if their ephemerides are not accurate enough, even if they are excellent targets for atmospheric characterization. Many currently known planets have large ephemeris uncertainties, and the analysis by Dragomir et al. (2019) suggests many *TESS* targets will have errors of more than 30 min less than a year after discovery due to the short baseline of *TESS* observations. To maintain, and verify, the ephemerides of these planets will require follow-up observations over the coming years from the ground and space.

Given the brightness of the host stars and the large transit depths of many of these planets, modestly sized telescopes can play a crucial role in this activity. To achieve regular observations of all known exoplanets, telescope time must be efficiently utilised. As it is not always clear when the most recent observations of a target occurred, follow-up observations need to be coordinated to maximize the effectiveness of the data. Community-wide citizen science efforts, such as the Exoplanet Transit Database and Exoplanet Timing Survey (Zellem et al. 2019) and ExoClock, need to be established to create a network of individuals and groups to monitor new discoveries. This need not be limited to citizen astronomers but should include all research groups with access to telescopes of all sizes. This organized and structured approach should build upon the work of existing schemes.

Researcher engagement with citizen astronomers, citizen science, and in educational outreach offers an excellent opportunity to support future space missions. Stimulating this engagement and devising a coordinated approach to maintaining exoplanet ephemerides will be imperative in the coming years. Projects such as the ETS, ExoClock, and ORBYTS need to become more widespread and methodical in their approach to transit follow-up (the selection of targets here was somewhat ad hoc and this is what needs to be avoided). Finally, it is critical that data from these observations are publicly available, especially for planets that display deviations in transit mid-time.

Here we homogeneously analyse the data but the reduction method has differed between observers which can lead to inconsistencies. The ETD provides a rating of the quality of the uploaded, from 1 to 5, but its vetting is perhaps not as extensive as other data bases, such as the Minor Planet Center. A systematic approach is required, with guidelines that ensure all data are processed in the correct manner. For exoplanet observations, the choice of comparison stars, the provision of correct timing, and overall consistency are paramount. Performing such quality checks on the data can be complex, requiring significant data storage and processing capabilities, but are critical if high-precision ephemerides are to be obtained. Thus future projects should allow the submission of raw images, along with the necessary calibration files, to allow for the data to homogeneously reduced and analysed, and, if an observer wishes to download data, the output format needs to be consistent to ensure efficacy. Being able to accept, and return, various data products from the raw frames to the light curve will increase the functionality of such a project. Alternatively, easy-to-use codes that automatically process the data without the need for human input (e.g. in the choice of comparison stars) could be used. ExoClock is expected to be expanded to provide such a platform for planets that could potentially be studied by *Ariel*.

8 CONCLUSIONS

We present follow-up observations of eight exoplanets with large uncertainties in their predicted transit time via a network of robotic ground-based telescopes and data from *TESS*. We refine the ephemeris data for these planets and, for seven of them, find that the observed transit time was outside the predicted uncertainties. This can only be mitigated for by regularly following up targets and, given the number of planets that are expected to be detected in the coming years, such an effort will require a large amount of telescope time. Therefore, a coordinated approach is required and citizen astronomers and educational outreach provide an excellent opportunity to contribute towards this effort. Schemes that stimulate this engagement will be crucial in maintaining transit times for the next generation of telescopes.

ACKNOWLEDGEMENTS

The authors wish to thank Dr Ehsan Pedram from Preston Manor School and Martin Yates from Beal High School for their dedication in organizing the outreach sessions, devoting their spare time for the benefit of their students. We also thank Telescope Live for kindly proving access to their telescope network, without which this project would not have been possible. Access to the LCO network was provided to the ORBYTS programme by the Faulkes Telescope Project, which is coordinated by Cardiff University and Swansea University. Additionally, we thank Paul Edwards for supplying data storage solutions. This paper includes data collected by the *TESS* mission, which is funded by the NASA Explorer Program. *TESS* data are publicly available via the Mikulski Archive for Space Telescopes (MAST). This research has also used the NASA Exoplanet Archive, which is operated by the California Institute of Technology, under contract with the National Aeronautics and Space Administration through the Exoplanet Exploration Program. This work has been funded through the European Union's Horizon 2020 research and innovation programme (grant agreement no. 758892, ExoAI), and with the STFC grants ST/P000282/1, ST/P002153/1, ST/S002634/1, and ST/T001836/1. Finally, we thank the MAPS Faculty at UCL for their partial funding of the ORBYTS programme.

REFERENCES

Agol E., Steffen J., Sari R., Clarkson W., 2005, MNRAS, 359, 567
Akeson R. L. et al., 2013, PASP, 125, 989
Alonso R. et al., 2014, A&A, 567, A112
Anderson D. R. et al., 2012, MNRAS, 422, 1988
Barclay T., Pepper J., Quintana E. V., 2018, ApJS, 239, 15
Benneke B. et al., 2017, ApJ, 834, 187
Bouma L. G. et al., 2019, AJ, 157, 217
Brandl B. R. et al., 2018, in Evans C. J., Simard L., Takami H., eds, Proc. SPIE Conf. Ser. Vol. 10702, Ground-Based and Airborne Instrumentation for Astronomy VII. SPIE, Bellingham, p. 107021U
Burdanov A. et al., 2018, PASP, 130, 074401
Changeat Q., Edwards B., Waldmann I. P., Tinetti G., 2019, ApJ, 886, 39
Chubb K. L. et al., 2018a, J. Quant. Spec. Radiat. Transf., 204, 42
Chubb K. L. et al., 2018b, J. Quant. Spec. Radiat. Transf., 218, 178
Claret A., Hauschildt P. H., Witte S., 2012, A&A, 546, A14
Claret A., Hauschildt P. H., Witte S., 2013, A&A, 552, A16
Darby-Lewis D. et al., 2019, J. Mol. Spectrosc., 362, 69
Dragomir D., Harris M., Pepper J., Barclay T., Villanueva Steven J., 2019, AJ, 159, 219,
Eastman J., Siverd R., Gaudi B. S., 2010, PASP, 122, 935
Edwards B., Savini G., Tinetti G., Tessenyi M., Arena C., Lindsay S., Bowles N., 2019a, J. Astron. Telesc. Instrum. Syst., 5, 014006
Edwards B., Lindsay S., Savini G., Tinetti G., Arena C., Bowles N., Tessenyi M., 2019b, J. Astron. Telesc. Instrum. Syst., 5, 034004
Edwards B. et al., 2019c, Exp. Astron., 47, 29
Edwards B., Mugnai L., Tinetti G., Pascale E., Sarkar S., 2019d, AJ, 157, 242
Fanson J. et al., 2018, in Marshall H. K., Spyromilio J., eds, Proc. SPIE Conf. Ser. Vol. 10700, Ground-based and Airborne Telescopes VII. SPIE, Bellingham, p. 14
Fridlund M. et al., 2010, A&A, 512, A14
Greene T. P., Line M. R., Montero C., Fortney J. J., Lustig-Yaeger J., Luther K., 2016, ApJ, 817, 17
Hellier C. et al., 2015, AJ, 150, 18
Hippke M., David T. J., Mulders G. D., Heller R., 2019, AJ, 158, 143
Kabath P., Skarka M., Sabotta S., Guenther E., 2019, Contrib. Astron. Obs. Skalnaté Ples, 49, 462
Kawashima Y., Hu R., Ikoma M., 2019, ApJ, 876, L5
McKemmish L. K., Chubb K. L., Rivlin T., Baker J. S., Gorman M. N., Heward A., Dunn W., Tessenyi M., 2017a, Astron. Geophys., 58, 5.11
McKemmish L. K. et al., 2017b, ApJS, 228, 15
McKemmish L. K. et al., 2018, ApJ, 867, 33
Maciejewski G. et al., 2016, A&A, 588, L6
Mackebrandt F. et al., 2017, A&A, 608, A26
Mallonn M. et al., 2019, A&A, 622, A81
Maxted P. F. L. et al., 2016, A&A, 591, A55
Mortier A., Santos N. C., Sousa S. G., Fernand es J. M., Adibekyan V. Z., Delgado Mena E., Montalto M., Israelian G., 2013, A&A, 558, A106
Poddaný S., Brát L., Pejcha O., 2010, New Astron., 15, 297
Raetz S., Heras A. M., Fernández M., Casanova V., Marka C., 2019, MNRAS, 483, 824
Rauer H., Aerts C., Cabrera J., PLATO Team, 2016, Astron. Nachr., 337, 961
Ricker G. R. et al., 2014, in MacEwen H. A., Fazio G. G., Lystrup M., Batalha N., Siegler N., Tong E. C., eds, Proc. SPIE Conf. Ser. Vol. 9143, Space Telescopes and Instrumentation 2014: Optical, Infrared, and Millimeter Wave. SPIE, Bellingham, p. 15
Rocchetto M., Waldmann I. P., Venot O., Lagage P. O., Tinetti G., 2016, ApJ, 833, 120
Rodler F., 2018, Exoplanet Research in the Era of the Extremely Large Telescope (ELT). Springer, New York, USA
Rodriguez J. E. et al., 2016, AJ, 151, 138
Skidmore W., Anupama G. C., Srianand R., 2018, The Thirty Meter Telescope International Observatory facilitating transformative astrophysical science, CURRENT SCIENCE, VOL. 113, NO. 4, 25 AUGUST 2017, preprint (arXiv:1806.02481)
Smith A. M. S. et al., 2018, actaa, 69, 135
Soto M. G. et al., 2018, MNRAS, 478, 5356
Sousa-Silva C., McKemmish L. K., Chubb K. L., Baker J., Barton E. J., Gorman M. N., Rivlin T., Tennyson J., 2018, Phys. Educ., 53, 015020
Southworth J., 2011, MNRAS, 417, 2166
Sullivan P. W. et al., 2015, ApJ, 809, 77
Tinetti G. et al., 2018, Exp. Astron., 46, 135
Tsiaras A., Waldmann I. P., Rocchetto M., Varley R., Morello G., Damiano M., Tinetti G., 2016, Astrophysics Source Code Library, record ascl:1612.018
Turner O. D. et al., 2016, PASP, 128, 064401
Wheatley P. J. et al., 2018, MNRAS, 475, 4476
Zellem R. T. et al., 2019, Bull. Am. Astron. Soc., 51, 416

[1]*Department of Physics and Astronomy, University College London, Gower Street, London WC1E 6BT, UK*
[2]*Department of Physics (Atmospheric, Oceanic and Planetary Physics), University of Oxford, Parks Rd, Oxford OX1 3PU, UK*
[3]*Preston Manor High School, Carlton Avenue East, Wembley HA9 8NA, UK*
[4]*Beal High School, Woodford Bridge Road, Ilford, Essex IG4 5LP, UK*
[5]*Royal Observatory Greenwich, Greenwich, London SE10 8XJ, UK*
[6]*Birkbeck, University of London, Malet Street, London WC1E 7HX, UK*

[7]*Spaceflux Ltd., 71-75 Shelton Street, Covent Garden, London WC2H 9JQ, UK*
[8]*Leibniz-Institut für Astrophysik Potsdam, An der Sternwarte 16, D-14482 Potsdam, Germany*
[9]*Club d'Astronomie de Wittelsheim, 68375 Wittelsheim, France*
[10]*Santa Maria de Montmagastrell Remote Observatory, E-25300 Tarrega, Spain*
[11] *Observatory of Baronnies Provençales, F-05150 Moydans, France*
[12]*Observatoire SADR Chili, 8320000 Santiago, Chile*
[13]*Les Barres Observatory, 12113 Lamanon, France*
[14]*Facultad de Ciencias Astronómicas y Geofísicas, Universidad Nacional de La Plata, Paseo del Bosque, S/N-1900 La Plata, Argentina*
[15]*Instituto de Astrofísica de La Plata (CCT La Plata – CONICET/UNLP), S/N-1900 La Plata, Argentina*
[16]*Rarotonga Observatory, Rarotonga, Cook Islands*
[17]*El Sauce Observatory, Coquimbo Province, 1780000 Río Hurtado, Chile*
[18]*Observatori Astronómic Albanyá, Camí de Bassegoda, E-17733 Girona, Spain*
[19]*Observatory Ca l'Ou, San Martí Sesgueioles, E-08008 Catalonia, Spain*
[20]*National Youth Space Center, Goheung, Jeollanam-do 59567, Republic of Korea*
[21]*OPERA Observatory, F-33820 Saint Palais, France*
[22]*Observatory of Josef Sadil, Havlíčkova 514, CZ-264 01 Sedlčany, Czech Republic*
[23]*Observatorio de Elche, E-03202 Elche, Spain*
[24]*Taurus Hill Observatory, FI-79480 Kangaslampi, Finland*
[25]*Observatoire de Vaison la Romaine, Au Palis, F-84110 Vaison la Romaine, France*
[26]*Anunaki Observatory, E-28410 Manzanares El Real, Spain*
[27]*Montcabrer Observatory, 03004 Alicante, Spain*
[28]*Raetz Observatory, Stiller Berg 6, D-98587 Herges-Hallenberg, Germany*
[29]*International Citizen Observatory, Munich, D-80939, Germany*
[30]*British Astronomical Association, Burlington House, Piccadilly, London W1J 0DU, UK*
[31]*Variable Star and Exoplanet Section of Czech Astronomical Society, Vsetínská 941/78, CZ-757 01 Valašské Meziříčí, Czech Republic*
[32]*Blue Skies Space Ltd., 69 Wilson Street, London EC2A 2BB, UK*
[33]*University College London Observatory, Mill Hill, London NW7 2QS, UK*

This paper has been typeset from a TEX/LATEX file prepared by the author.